# Structural and Antibacterial Studies of Hydrothermally SynthesizedCu Substituted Zn Nanoparticles

PradeepRajuBadabagni[a], DevannaNayakanti[b]

[a]Research Scholar, Jawaharlal Nehru Technological University Anantapur, Ananthapuramu

[b]JNTUA College of Engineering, Ananthapuramu, Constituent college of Jawaharlal Nehru Technological University Anantapur, Ananthapuramu

Corresponding Author Mail: pradeepraju.b@gmail.com

## Abstract

Hydrothermal technique has been used to create nanocrystalline powders of copper substituted zinc ferrite with general formula $Zn_{1-x}Cu_xFe_2O_4$(x = 0.2, 0.4, 0.6, and 0.8). The synthesised samples are recognised by powder X-ray diffraction, which showed prominent peaks due to its considerable crystalline nature. Crystallite size has been determined, and structural analysis shows their cubic nature and remarkable crystalline. Measurements made with FT-IR in the 4000-400 cm-1 range help to clarify the existence of functional groups. Selected Gram negative (Proteus vulgaris) and Gram positive (Bacillus subtilis) bacterial strains were used to test the nanocrystalline powders' antibacterial properties. The incorporation of Cu into Zn ferrite nanoparticles results in an increase in activity. These materials, which have enhanced structural and antibacterial qualities, can be used in hygiene, medicines, and the textile sector.

**Keywords:**Nanoparticles; X-Ray Diffraction; Crystallite Size; Antibacterial Activity;

## 1. Introduction

Due to their diversity in electrical, magnetic, and antibacterial properties, copper replaced zinc ferrites nanoparticles are attracting more and more interest. Substantial industrial regions are capitalising on its numerous applications, which include magnetic read-write heads for high-speed digital tape or disc recording transformer cores, rod antennas, [1, 2], radar-absorbing materials [3, 4], and as a highly effective catalyst for organic or inorganic processes. [5, 6]. Because they have a high resistance and a low dielectric loss, they can be used for these things.Using their magnetic properties, biological compatibility, or antibacterial properties, Cu-Zn nanoparticles can be functionalized to provide magnetically targeted medicines for biomedical purposes [4,5].

1352

*Eur. Chem. Bull.* **2023**,*12(3), 1352-1364*

Due to their unique properties, magnetic nanoparticles used in biomedical applications need to be carefully controlled in terms of their size, shape, distribution, and the conditions that affect these factors. Stabilizing the dispersion of magnetic nanoparticles in water is theoretically required. As a first step towards creating biocompatible nanoparticles, scientists often encapsulate magnetic nanoparticles with a polymer shell made of PEG, Chitosan, phospholipids, dextran, or polyethyleneimine[6]. To improve the dispersion of colloidal particles and control their sizes, Buteica et al. [7] created magnetic, core-shelled $Fe_3O_4$ nanoparticles. The $Fe_3O_4$ nanoparticles were coated with oleic acid, a surfactant, followed by the addition of four antibiotics as an adsorption coating (cephalosporins). Both Escherichia coli (E. coli) and Staphylococcus aureus were employed to explore how bacteria function (S. aureus).The inhibition zone widths for cephalosporins were found to be larger than those for cephalosporin-nanofluid for the same time span. The antibiotic was only transported via the nanofluid.

Also, when an antibiotic is targeted at certain organs like the kidney and brain, small magnetic nanoparticles enable delivery of the medication. Sun et al.'s[8] thermal decomposition technique produced $Fe_3O_4$ nanoparticles by combining an iron salt with 1,2-hexadecanediol, oleic acid, oleylamine, and biphenyl ether. The antibacterial properties of the $Fe_3O_4$ nanoparticles were subsequently improved by coating them in silver. With an external magnetic field, the nanostructures could be recovered and reused because of their paramagnetic properties. In order to improve the nanopowders' qualities, it is vital to have precise control over their homogeneity, elemental content, and powder shape. This is made possible by uniformly dispersed nano-sized metal clusters. The hydrothermal procedure is a good substitute for other established techniques for creating ceramic oxide composites because of these benefits [9].

With $Fe^{3+}$ evenly distributed between tetrahedral and octahedral sites and $Zn^{2+}$ in octahedral sites, zinc ferrite displays an inverted spinel structure. $Zn^{2+}$ is found in tetrahedral and $Fe^{3+}$ is found in octahedral sites in the combination $ZnFe_2O_4$, which exhibits a typical spinel structure [10]. Consequently, depending on the concentration of the precursor solutions, copper substitution in $ZnFe_2O_4$ may result in a deformed spinel structure. There aren't many studies that look at how copper content affects the magnetic and microstructural characteristics of copper-substituted zinc ferrite nanopowders [11]. According to one study, the types of cations present and how they are distributed throughout the spinel lattice's two interstitial sites affect the mineral's magnetic characteristics [12]. Another asserted that the Curie temperature

1353

*Eur. Chem. Bull.* **2023**,*12(3), 1352-1364*

of the ferrite was lowered by replacing $Fe^{3+}$ with $Cu^{2+}$ [13, 14]. The application of these magnetic nanopowders in the biological field, however, has not been discussed in any reports.

The goal of this study was to come up with new nanopowders made of iron that are magnetic and can also kill bacteria. This was done so that a drug delivery system could work and so that less antibiotics would be needed. To do this, we made zinc-substituted cobalt ferrite nanopowders using the hydrothermal method and citric acid (CA) as a chelating agent. Copper substitution was carefully looked at to see how it changed the zinc ferrite nanopowders' surface morphology, size distribution, surface wetting, surface roughness, and antibacterial properties.

## 2. Materials and methods

Fine powders with general formula $Zn_{1-x}Cu_xFe_2O_4$ (x = 0.2, 0.4, 0.6 and 0.8), hereinafter denoted as ZCF0.2,ZCF0.4,ZCF0.6 and ZCF0.8and were obtained by hydrothermal method. The metal nitrate solutions $Fe(NO_3)_3.9H_2O$ (99.9%, Aldrich)$Zn(NO_3)_2.6H_2O$(99.9%, Aldrich)and $Cu(NO_3)_2.6H_2O$(99.9%, Aldrich) were mixed in stoichiometric proportions in double distilled water. For the $Zn_{1-x}Cu_xFe_2O_4$synthesis the following chemical equations could be written:

$$Zn(NO_3)_2.6H_2O+Cu(NO_3)_2.6H_2O+Fe(NO_3)_3.9H_2O \rightarrow ZnCuFe_2O_4+ 10HNO_3+25H_2O+1/2O_2$$
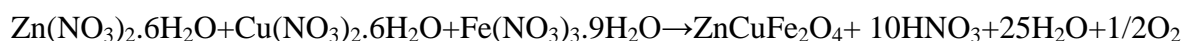
The aforementioned solution was vigorously agitated for approximately two hours, after which the homogenous mixture was put into a 40 mL teflon-lined autoclave. The autoclave was then tightly sealed and heated at 150°C for eight hours in an oven. The autoclave was then given time to cool to ambient temperature. After being separated by centrifugation, the solid products were repeatedly rinsed in distilled water and ethanol before being dried for six hours at 60 degrees Celsius. The last products, solid ones, were attained [15–20]. Using X-ray diffraction (XRD), a Seifert diffractometer (XRD 3003 PTS type) with Cu-K radiation (l = 1.5405), crystal structure analysis (crystallite size, lattice parameter estimation, and single-phase identification) was done for 2 ranging from 100 to 900. At room temperature, FTIR data was recorded using a Jasco 660 Plus Spectrophotometer with the KBr pellet method and wavenumbers between 4000 and 400 cm$^{-1}$. Using a vibrating sample magnetometer system, the produced samples' magnetic characteristics were investigated at room temperature (VSM 3900 Princeton). It was also investigated how the replacement of Cu for Zn affected the magnetic characteristics. Also, the coercive field fluctuations with x values as well as the maximum values of the magnetization (Mmax), remanent magnetizations (Mr), and magnetizations were examined. Using the rapid and simple agar diffusion method, the antibacterial activity of CuxZn1-xFe$_2$O$_4$ (x = 0.2, 0.4, 0.6 and 0.8) nanoparticles was determined. For this experiment,

1354

*Eur. Chem. Bull.* ***2023****,12(3), 1352-1364*

gramme positive Bacillus subtilis and gramme negative Proteus vulgaris bacteria were chosen. Standard bacterial strains were cultivated on Nutrient Agar medium and let to sit for 24 hours while being kept at 37 °C. Bacterial suspensions were made from the bacterial colonies culture after an incubation period [21]. To make sure the bacteria grew evenly, a hemocytometer was used to make bacterial solutions with 106 CFU/ml. These solutions were then spread out over the surface of nutrient agar plates with 0.066, 0.66, and 6.66 mg.ml-1 of Cu nanoparticles. After 24 and 48 hours of growth at 37°C, the number of colonies was counted.

## 3. Results and Discussion

### 3.1. XRD analysis

Fig. 1 displays the Cu-Zn ferrites' XRD patterns. Each sample's diffraction pattern yielded the strongest reflection peak, which was mapped to the (3 1 1) XRD diffraction plan typical for the spinel phase. The XRD patterns show that the cubic structure of spinel formed in a single phase. All of the reflection peaks were found and indexed using the JCPDS 73-1963 database as a guide[22].
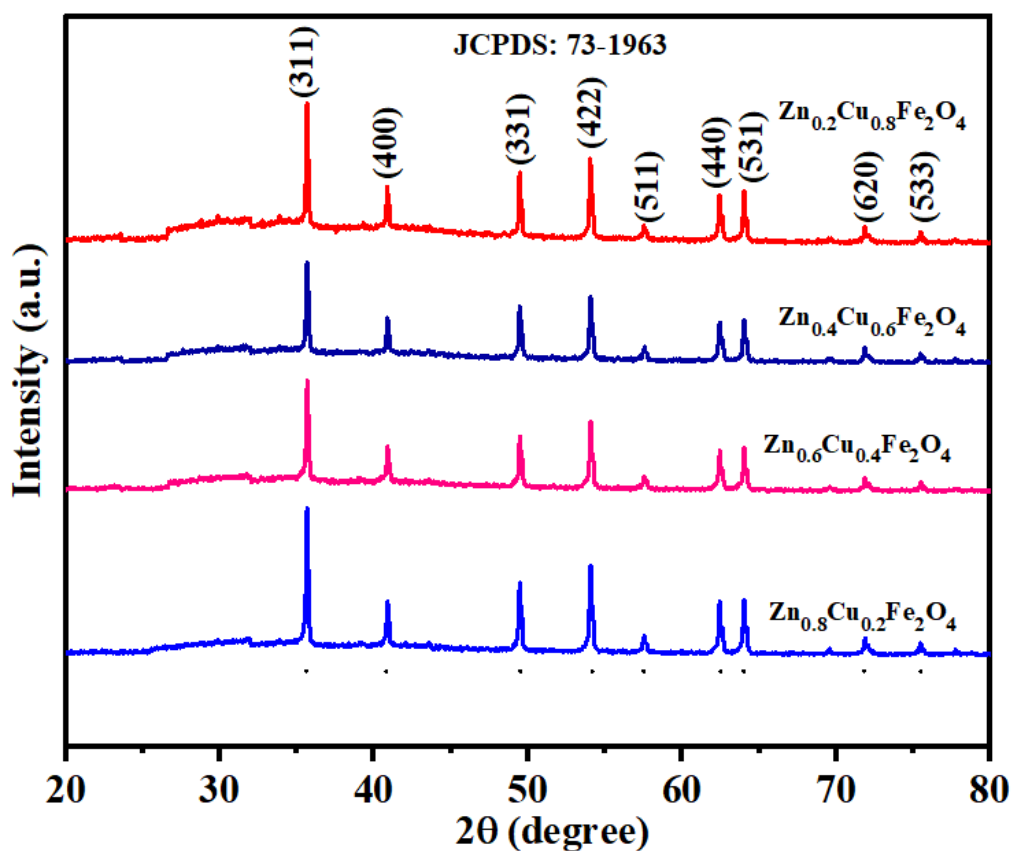


Figure 1: XRD patterns of $Zn_{1-x}Cu_xFe_2O_4$ (x=0.2-0.8) (ZCF) nanoparticles

1355

*Eur. Chem. Bull. 2023,12(3), 1352-1364*

The Debye-Scherrer formula was used to determine the crystallite size from peak broadening:

Dhkl= k/[(2 cos]

Where D is the crystallites' size, is the X-ray source's wavelength (Cu K, = 1.5405 ), (rad) is the peak's full width at half maximum (3 1 1), and is the diffraction angle. For $Zn_{1-x}Cu_xFe_2O_4$ (x = 0.2, 0.4, 0.6, and 0.8), the estimated crystallite sizes of the produced samples were determined to be 41.44, 45.12, 45.62, and 47.71 nm, respectively.

**3.2. SEM Analysis**

SEM was used to examine the morphological characteristics of produced ZCF nanoparticles. Figure 2 displays micrographs of the prepared samples after 600°C annealing. The spherical form of these nanoparticles was expressed along with homogenous dispersion and an average grain size of about 50 m. The fine granules may be the source of these enlarged spheres and microscopic spheres [22–25]. Due to the magnetic attraction of nanoparticles, these samples have uneven forms, cohesiveness of grains, and sizes, which might alter their biological activity and internalisation, such as an anti-bacterial effect. Because of their flat surface, synthesised nanoparticles can interact with bacterial cell walls. Moreover, due to their higher surface area, spherical nanoparticles of tiny size have improved anti-bacterial action in comparison to those of larger sizes [26–29].
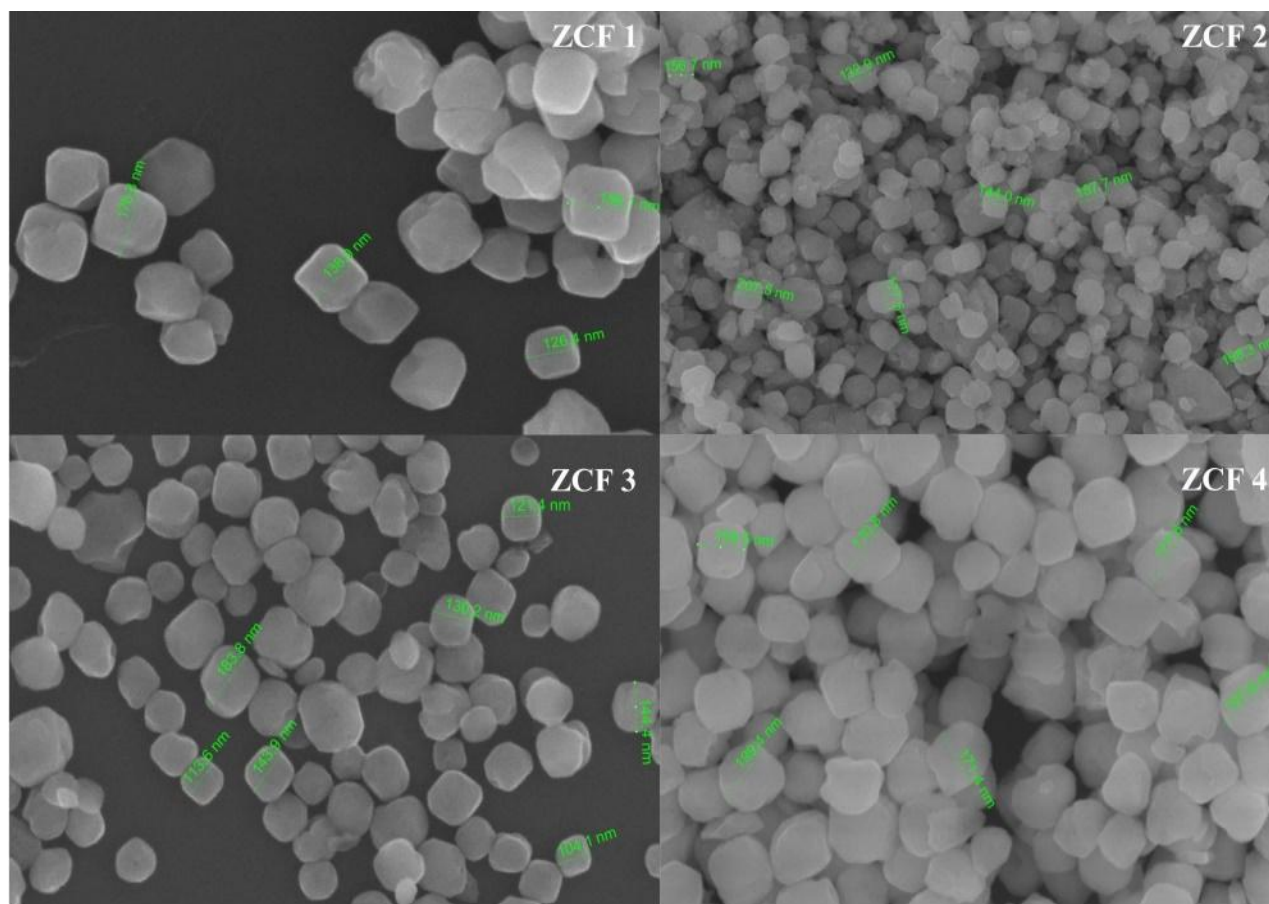
1356

*Eur. Chem. Bull. 2023,12(3), 1352-1364*

Figure 2: SEM pictures of $Zn_{1-x}Cu_xFe_2O_4$ (x=0.2-0.8) (ZCF) nanoparticles

### 3.3. FTIR Analysis

The type of the substance's molecular bonds and the existence of functional groups can be determined using FT-IR. The $Zn_{1-x}Cu_xFe_2O_4$ (x = 0.2, 0.4, 0.6, and 0.8) samples' FTIR spectra at room temperature were examined, and the results are given in Fig. 3 in the wavenumber range 400-4000 cm-1. All of the samples' recorded FTIR spectra show certain commonalities. It has six bands of absorption and was seen at wavelengths of 420, 509, 1328, 1642, 2344, and 3363 cm-1. The spectra show the two primary absorption peaks of spinel ferrite. The absorption band at 420 cm1 is caused by the stretching vibration of the Fe-O atoms when they are located in octahedral locations. The intrinsic stretching vibration of the tetrahedral sites of Zn-O is associated with the band of absorption that has a frequency of 509 cm-1. From these two absorption peaks, it is reasonable to draw the conclusion that the spinel-type structure is present in the material. According to Waldron [30], Lavat [30], and Baran [31], the inherent stretching vibrations of bonds between tetrahedral metal ions and oxygen ions are generally thought to be the cause of the greatest absorption peak in the region of 600-

1357

*Eur. Chem. Bull. 2023,12(3), 1352-1364*

400 cm-1. On the other hand, the weakest absorption peak is related to stretching vibrations of bonds between octahedral metal ions and oxygen ions. This phenomenon is responsible for the lowest level of absorption.The bands that are located at 1328 and 1642 cm1 demonstrate the stretching vibration of the C-H bond.The stretching and bending vibrations of the H-O-H bonds on the surface are responsible for other reasonable absorption peaks at 2344 and 3474cm-1 that are lesspronounced[32].



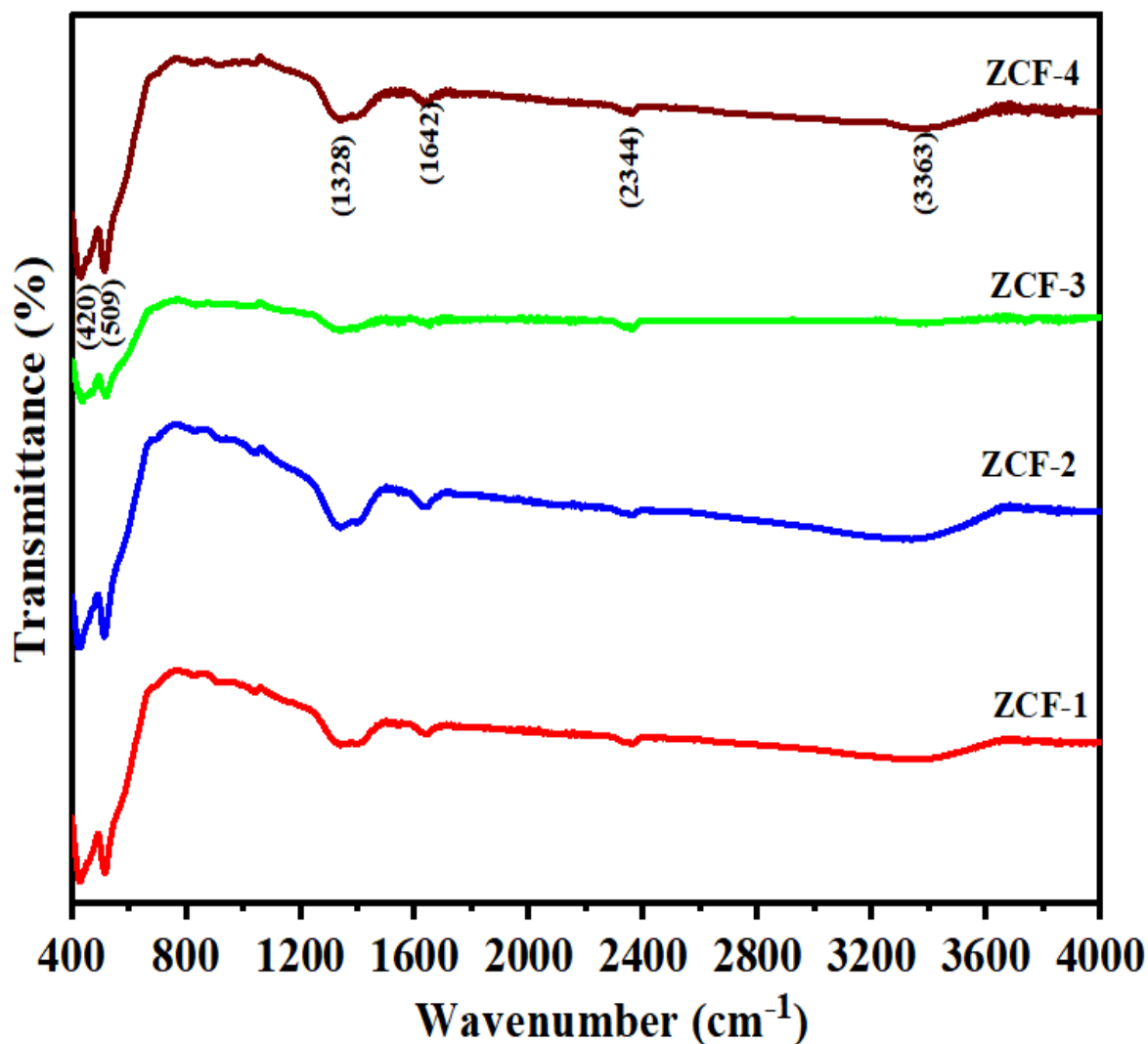Figure 3: FTIR spectra of $Zn_{1-x}Cu_xFe_2O_4$ (x=0.2-0.8) (ZCF) nanoparticles

## 3.4 Antimicrobial Activity

The bactericidal activity of ZCFnanoparticles was evaluated by subjecting gram-negative (Proteus vulgaris) and gram-positive (Bacillus subtilis) bacterial strains to a disc diffusion test.The absence of growth surrounding the nanoparticle is an indirect measure of the ability of ferrites to inhibit the growth of bacteria. Based on findings in table 1 and Figure 4

1358

*Eur. Chem. Bull.* **2023**,*12(3), 1352-1364*

Proteus vulgaris, Bacillus subtilis could be killed by prepared nanoparticles, in addition, the nanoparticles exhibit their antibacterial effects to a greater extent in Proteus vulgaris and Bacillus subtilis bacterial strains[33]. Uniquearrangements of lipid, peptidoglycans with less than 15nm thickness and lipopolysaccharides have been seen in gram negative bacteria. While in gram positive bacteria structure, there are mainly very thick peptidoglycans with cell walls that play the important role of a boundary to protect proteins so that they can easily leak out when the cell membrane is damaged[34-35]. Our experimental results showed that preparednanoparticles can disruption of cell membrane in both Gram-positive and Gram-negative strains, and can lead to cell membrane damage followed by bacterial death.
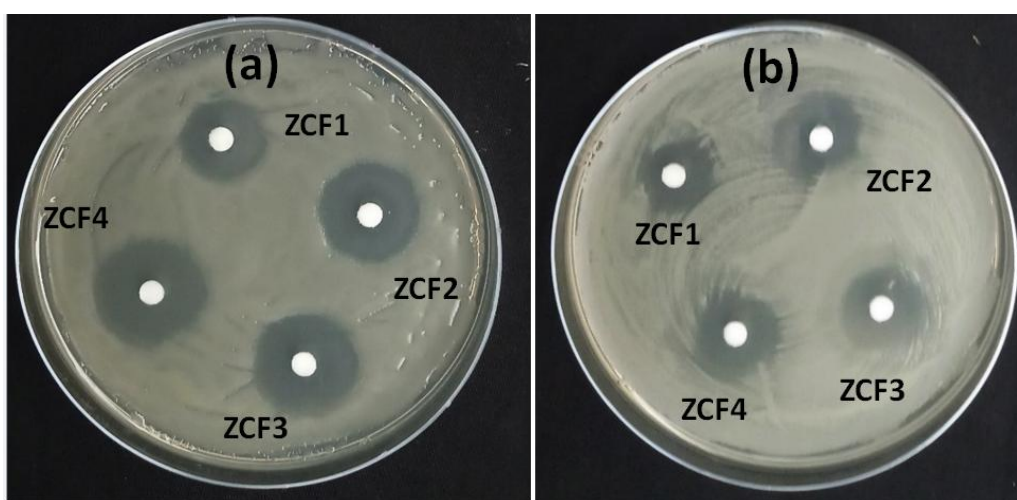


Figure 4: Antibacterial activities of Zinc Copper Ferrite nanoparticles against (a) Proteus vulgaris and (b) Bacillus subtilis via Kirby–Bauer disk diffusion technique.

**Table 1:Antibacterial activities of Zinc Copper Ferrite nanoparticles via Kirby–Bauer disk diffusion technique.**

| | | Inhibition Zone (cm) | |
|---|---|---|---|
| S.No | Compound | Bacillus subtilis (Gram positive) | Proteus vulgaris (Gram negative) |
| 1 | ZCF-1 | 1.3±0.2 | 1±0.2 |
| 2 | ZCF-2 | 1.6±0.3 | 1.3±0.2 |
| 3 | ZCF-3 | 2.1±0.2 | 1.5±0.3 |
| 4 | ZCF-4 | 2.2±0.1 | 2.0±.2 |

1359

*Eur. Chem. Bull.* **2023**,*12(3), 1352-1364*

**3.5 Conclusions:**

The type of the substance's molecular bonds and the existence of functional groups can be determined using FT-IR. The $Zn_{1-x}Cu_xFe_2O_4$ (x = 0.2, 0.4, 0.6, and 0.8) samples' FTIR spectra at room temperature were examined, and the results are given in Fig. 3 in the wavenumber range 400-4000 cm-1. All of the samples' recorded FTIR spectra show certain commonalities. It has six bands of absorption and was seen at wavelengths of 420, 509, 1328, 1642, 2344, and 3363 cm-1. The spectra show the two primary absorption peaks of spinel ferrite. The stretching vibration of Fe-O in octahedral sites is responsible for the absorption band at 420 cm1. The 509 cm-1 absorption band is related to the intrinsic stretching vibration of the tetrahedral sites of Zn-O. It may be possible to infer the existence of the spinel-type structure from these two absorption peaks. According to Waldron [30], Lavat [30], and Baran [31], Most people think that the strongest absorption peak between 600 and 400 cm-1 is caused by the stretching vibrations of the bonds between tetrahedral metal ions and oxygen ions.On the other hand, the stretching vibrations of bonds between octahedral metal ions and oxygen ions are thought to be responsible for the weakest absorption peak. The bands that are located at 1328 and 1642 cm1 demonstrate the stretching vibration of the C-H bond. Further tolerable absorption peaks may be found at 2344 and 3474cm-1, but they are not as prominent as the ones previously mentioned [32]. These peaks are caused by the stretching and bending vibrations of the H-O-H bonds on the surface.

**CONFLICT OF INTEREST**

The authors say that they don't have any interests that conflict with each other.

**References:**

[1]. M. Sorescu, L. Diamandescu, R. Swaminthan, M.E. McHenry, M. Feder, Structural and magnetic properties of NiZn and Zn ferrite thin films obtained by laser ablation deposition J. Appl. Phys. 97 (2005) 10G105.

[2]. U.R. Lima, M.C. Nasar, R.S. Nasar, M.C. Rezende, J.H. Araujo, Ni–Zn nanoferrite for radar-absorbing material, J. Magn. Magn.Mater.320 (2008) 1666.

[3]. J.-S. Kim, J.-R. Ahn, C.W. Lee, Y. Murakami, D. Shindo, J. Mater. Chem. 11 (2001) 3373.

[4]. A.M. Nowicka, A. Kowalczyk, M. Donten, P. Krysinski, Z. Stojek, Anal.Influence of a Magnetic Nanoparticle As a Drug Carrier on the Activity of Anticancer Drugs: Interactions of Double Stranded DNA and Doxorubicin Modified with a Carrier, Chem. 81 (2009) 7474.

1360

*Eur. Chem. Bull. 2023,12(3), 1352-1364*

[5]. B.K. Sunkara, R.D.K. Misra, Enhanced antibactericidal function of W4+-doped titania-coated nickel ferrite composite nanoparticles: A biomaterial system, ActaBiomater. 4 (2008) 27.

[6]. K.Byrappa, S. Ohara, and T. Adschiri, Nanoparticles synthesis using supercritical fluid technology - towards biomedical applications, Adv. Drug Delivery Rev. 60(3) (2008)299–327.

[7]. A. S. Buteica, D. E. Mihaiescu, A. M. Grumezescu, B. S. Vasile, A. Popescu, O. M. Mihaiescu, R. Cristescu, The antibacterial activity of magnetic nanofluid: Fe3O4/oleic acid/cephalosporins core/shell/adsorption shell proved on S. aureus and E. coli and possible applications as drug delivery systems, Dig. J. Nanomater. Bios. 5(4) (2010)927–932.

[8]. S. Sun, H. Zeng, D. B. Robinson, S. Raoux, P. M. Rice, S. X. Wang, and G. Li, Monodisperse $MFe_2O_4$ (M = Fe, Co, Mn) Nanoparticles, J. Am. Chem. Soc. 126(1) (2004) 273–279.

[9]. G. De, G. Mattei, P. Mazzoldi, C. Sada, G. Battaglin, and A. Quaranta, Au−Cu Alloy Nanocluster Doped $SiO_2$ Films by Sol−Gel Processing, Chem. Mater. 12(8) (2000)2157–2160.

[10]. Grigorova, M., Blythe, H.J., Blaskov, V., Rusanov, V., Petkov, V., Masheva, V., Nihtianova, D., Martinez, L.M., Muñoz, J.S., Mikhov, M.: Magnetic properties and Mössbauer spectra of nanosized $CoFe_3O4$ powders. J. Magn. Magn. Mater. 183, 163−172 (1998)

[11]. NoppakunSanpo, Christopher C. Berndt, James Wang, Microstructural and antibacterial properties of zinc-substituted cobalt ferrite nanopowders synthesized by sol-gel methods, Journal of Applied Physics 112 (2012) 084333.

[12]. P. Yaseneva, M. Bowker, and G. Hutchings, Structural and magnetic properties of Zn-substituted cobalt ferrites prepared by co-precipitation method, Phys. Chem. Chem. Phys. 13(41) (2011)18609–18614.

[13]. P. Pandya, H. Joshi, and R. Kulkarni, Bulk magnetic properties of Co-Zn ferrites prepared by the co-precipitation method, J. Mater. Sci. 26(20) (1991)5509–5512.

[14]. O. M. Hemeda, Electrical properties of the Co-Zn ferrites irradiated with γ-rays, Phase Transitions 51(1-2) (1994) 87–95.

1361

*Eur. Chem. Bull.* **2023**,*12(3), 1352-1364*

[15]. A.E. Lavat, E.J. Baran, IR-spectroscopic characterization of NaLn3TiO4 and AgLn3TiO4 oxides related to the K2NiF4 structural type, J. Alloys Compd. 419 (2006) 334.

[16]. N Suresh Kumar, R Padma Suvarna, K Rama Krishna Reddy, T Anil Babu, S Ramesh, B Venkata Shiva Reddy, H Manjunatha, K Chandra Babu Naidu, Tetragonal structure and dielectric behaviour of rare-earth substituted $La_{0.8}Co_{0.16-x}Eu_{0.04}Gd_xTiO_3$ (x= 0.04–0.16) nanorods, Materials Chemistry and Physics, 278 (2021) 125598

[17]. B. Venkata Shiva Reddy, N. Suresh Kumar, T. Anil Babu, S. Ramesh, K. Srinivas, K. Chandra Babu Naidu, Structure, morphology, dielectric, and impedance properties of (1-x) $(Al_{0.2}La_{0.8}TiO_3)$ + (x) $(CuTiO_3)$ (x = 0.2–0.8) nanocomposites, Journal of Materials Science: Materials in Electronics, 32 (2021) 21225–21236

[18]. P Ankoji, N Suresh Kumar, K Chandra Babu Naidu, B PradeepRaju, Structural and luminescence properties of $Dy^{3+}$-doped $La_2(MoO_4)_3$ phosphors. Applied Physics A, 127 (2021) 552

[19]. Prasun Banerjee, N. Suresh Kumar, Kadiyala Chandra Babu Naidu, A. Franco Jr. & RavinderDachepalli, Stability of 2D and 3D Perovskites Due to Inhibition of Light-Induced Decomposition, Journal of Electronic Materials, 49 (2020) 7072–7084

[20]. N. Suresh Kumar, R. Padma Suvarna, K. Chandra Babu Naidu, Negative dielectric behavior in tetragonal $La_{0.8}Co_{0.2-x}Eu_xTiO_3$ (x = 0.01–0.04) nanorods, Materials Characterization, 166 (2020) 110425

[21]. Tamara Slatineanu, Alexandra RalucaIordan, MirceaNicolaePalamaru, Ovidiu Florin Caltun, Synthesis and characterization of nanocrystalline Zn ferrites substituted with Ni, Materials Research Bulletin 46 (2011) 1455–1460.

[22]. Mallikarjuna, S. Ramesh, N. Suresh Kumar, K. Chandra Babu Naidu, K. VenkataRatnam, H. Manjunatha, B. ParvatheeswaraRao, Structural transformation and high negative dielectric constant behaviour in (1-x) $(Al_{0.2}La_{0.8}TiO_3)$ + (x) $(BiFeO_3)$ (x = 0.2 - 0.8) nanocomposites, PhysicaE: Low-dimensional Systems and Nanostructures, 122 (2020) 114204

[23]. A. Mallikarjuna, S. Ramesh, N. Suresh Kumar, K. Chandra Babu Naidu, K. VenkataRatnam, H. Manjunatha, Photocatalytic activity, negative ac- electrical conductivity, dielectric modulus and impedance properties in 0.6 $(Al_{0.2}La_{0.8}TiO_3)$ +

1362

*Eur. Chem. Bull. 2023,12(3), 1352-1364*

0.4 ($BiFeO_3$) nanocomposite, Crystal Research and Technology, (2020) 202000068 (pp.1-10)

[24]. N. Suresh Kumar, R. Padma Suvarna, K. Chandra Babu Naidu, Microwave Heated Lead Cobalt Titanate Nanoparticles Synthesized by Sol-Gel Technique: Structural, Morphological, Dielectric, Impedance and Ferroelectric Properties, Materials Science and Engineering B 242 (2019) 23-30

[25]. Venkata Shiva Reddy, K. Srinivas, N. Suresh Kumar, K. Chandra Babu Naidu, S. Ramesh, Nanorods like microstructure, photocatalytic activity and ac-electrical properties of (1-x) ($Al_{0.2}La_{0.8}TiO_3$)+(x)($BaTiO_3$) (x = 0.2, 0.4, 0.6 & 0.8) nanocomposites, Chemical Physics Letters, 752 (2020) 137552

[26]. N. Suresh Kumar, R. Padma Suvarna, K. Chandra Babu Naidu, Structural and ferroelectric properties of microwave heated lead cobalt titanate nanoparticles synthesized by sol–gel technique, Journal Material Science: Materials in Electronics 29 (2018) 4738-4742

[27]. N. Suresh Kumar, R. Padma Suvarna, K. Chandra Babu Naidu, Sol-Gel Synthesized and Microwave Heated $Pb_{0.8-y}La_yCo_{0.2}TiO_3$ (y = 0.2–0.8) Nanoparticles: Structural, Morphological and Dielectric Properties, Ceramics International 44 (2018) 18189-18199

[28]. N. Suresh Kumar, R. Padma Suvarna, K. Chandra Babu Naidu, G. R. Kumar, S. Ramesh, Structural and functional properties of sol-gel synthesized and microwave heated $Pb_{0.8}Co_{0.2-z}La_zTiO_3$ (z = 0.05–0.2) nanoparticles, Ceramics International 44 (2018) 19408-19420

[29]. K. Chandra Babu Naidu, V. Narasimha Reddy, T. SofiSarmash, N. Suresh Kumar, T. Subbarao, Structural, Morphological, Optical, Electrical, Impedance and Ferroelectric Properties of BaO-ZnO-TiO2 Ternary System, Journal of The Australian Ceramic Society 55 (2019) 201-218

[30]. R.D. Waldron, Infrared Spectra of Ferrites, Phys. Rev. 99 (1955) 1727.

[31]. A.E. Lavat, E.J. Baran, X-ray diffraction and IR spectroscopic characterization of AgLnI3TiO4 oxides related to the K2NiF4 structural type, J. Alloys Compd. 368 (2004) 130.

[32]. P. AnnieVinosha, L.AnselMely, J.EmimaJeronsia, S.Krishnan, S.Jerome Das, Optik 134(2017) 99-108.

1363

*Eur. Chem. Bull. 2023,12(3), 1352-1364*

[33]. CH V, Chandra Babu NaiduK, C CS, Dachepalli R. Magnetic and antimicrobialproperties of cobalt-zinc ferrite nanoparticlessynthesized by citrate‐ gel method. Int J ApplCeramTechnol. 2019;00:1–10.

[34]. Ansari, M. A., Baykal, A., Asiri, S., &Rehman, S. Synthesis and Characterization of Antibacterial Activity of Spinel Chromium-Substituted Copper Ferrite Nanoparticles for Biomedical Application. Journal of Inorganic and Organometallic Polymers and Materials. 2018.

[35]. ReihanehHaghniaz, AtiyaRabbani, FereshtehVajhadin, Taous Khan, RozinaKousar, Abdul Rehman Khan, HosseinMontazerian, JavedIqbal, Alberto Libanori, Han‐ Jun Kimand Fazli Wahid, Journal of Nanobiotechnology, 2021, 1-15.

1364

*Eur. Chem. Bull. 2023,12(3), 1352-1364*